Eur. Phys. J. A (2021) 57:248
https://doi.org/10.1140/epja/s10050-021-00557-x

THE EUROPEAN PHYSICAL JOURNAL A

Regular Article - Experimental Physics

Experimental consolidation and absolute measurement of the $^{nat}C(p,x)^{11}C$ nuclear activation cross section at 100 MeV for particle therapy physics

Claus Maximilian Bäcker[1,2,3,4,a], Felix Horst[5,6], Wihan Adi[7], Christian Bäumer[1,2,3,4,8], Marcel Gerhardt[1], Walter Jentzen[4,9], Sandra Laura Kazek[4,9], Kevin Kröninger[1], Christoph Schuy[5], Nico Verbeek[2,3,4,10], Jens Weingarten[1], Jörg Wulff[2,3,4,6], Beate Timmermann[2,3,4,8,11]

[1] Faculty of Physics, TU Dortmund University, Otto-Hahn-Str. 4a, 44227 Dortmund, Germany
[2] West German Proton Therapy Centre Essen, Am Mühlenbach 1, 45147 Essen, Germany
[3] West German Cancer Center, Hufelandstr. 55, 45147 Essen, Germany
[4] University Hospital Essen, Hufelandstr. 55, 45147 Essen, Germany
[5] GSI Helmholtzzentrum für Schwerionenforschung, 64291 Darmstadt, Germany
[6] Institute of Medical Physics and Radiation Protection, THM University of Applied Sciences Giessen, 35390 Giessen, Germany
[7] Justus-Liebig-University Giessen, Heinrich-Buff-Ring 16, 35392 Giessen, Germany
[8] German Cancer Consortium (DKTK), Heidelberg, Germany
[9] Clinic for Nuclear Medicine, University Hospital Essen, Hufelandstr. 55, 45147 Essen, Germany
[10] University Duisburg Essen, Universitätsstr. 2, 45141 Essen, Germany
[11] Department of Particle Therapy, University Hospital Essen, Hufelandstr. 55, 45147 Essen, Germany

Received: 25 March 2021 / Accepted: 19 July 2021 / Published online: 2 August 2021

Communicated by Navin Alahari

Abstract The $^{nat}C(p,x)^{11}C$ reaction has been discussed in detail in the past [EXFOR database, Otuka et al. (Nuclear Data Sheets 120:272–276, 2014)]. However, measured activation cross sections by independent experiments are up to 15% apart. The aim of this study is to investigate underlying reasons for these observed discrepancies between different experiments and to determine a new consensus reference cross section at 100 MeV. Therefore, the experimental methods described in the two recent publications [Horst et al. (Phys Med Biol https://doi.org/10.1088/1361-6560/ab4511, 2019) and Bäcker et al. (Nuclear Instrum Methods Phys Res B 454:50–55, 2019)] are compared in detail and all experimental parameters are investigated for their impact on the results. For this purpose, a series of new experiments is performed. With the results of the experiments a new reference cross section of (68±3) mb is derived at (97±3) MeV proton energy. This value combined with the reliably measured excitation function could provide accurate cross section values for the energy region of proton therapy. Because of the well-known gamma-ray spectrometer used and the well-defined beam characteristics of the treatment machine at the proton therapy center, the experimental uncertainties on the absolute cross section could be reduced to 3%. Additionally, this setup is compared to the in-beam measurement setup from the second study presented in the literature (Horst et al. 2019). Another independent validation of the measurements is performed with a PET scanner.

1 Introduction

The activation of natural carbon and the production of the radionuclide ^{11}C by protons ($^{nat}C(p,x)^{11}C$) is a well studied nuclear reaction and measured cross sections are available from the threshold (18.72 MeV) up to several GeV [31]. However, the absolute cross section values vary by about 15% among the literature references and accumulate around two distinct trends. Interestingly, this difference still persists in three recent publications [5,6,17] where the $^{nat}C(p,x)^{11}C$ reaction has been studied independently with two different experimental setups.

In the past, the investigation of this reaction was motivated by the application as a monitor reaction for nuclear physics experiments, e.g. for the determination of the number of protons (e.g. Ref. [33]). Today, the interest on the $^{nat}C(p,x)^{11}C$

Supplementary Information The online version contains supplementary material available at https://doi.org/10.1140/epja/s10050-021-00557-x.

[a] e-mail: clausmaximilian.baecker@tu-dortmund.de (corresponding author)

reaction is motivated by its potential application in monitoring and verification of proton therapy. On the one hand, carbon is a main component of biological molecules. Therefore, ^{11}C is produced in the irradiated tissue as a by-product of the radiotherapy with protons or heavy ions and its spatial distribution can be determined with a positron emission tomography (PET) camera during or after the treatment [32]. On the other hand, dosimetry of proton fields with activated graphite foils has been proposed as an alternative approach to ionization chamber based dosimetry [28]. Such applications in medical physics require an accurate knowledge of the ^{nat}C(p,x)^{11}C cross section in the therapeutic energy range (proton energies up to 250 MeV) and suitable uncertainties for the accuracy required for radiotherapy. Monte Carlo transport codes are typically verified and optimized by comparison with experimental cross section data [4].

The goal of the presented study is to investigate the cause of the systematic deviations of measured ^{nat}C(p,x)^{11}C cross sections and to provide a consensus value at 100 MeV. For this purpose a comparative measurement using two different experimental methods, that from Dortmund / Essen [5,6], which is further called *Dortmund Low Background Facility (DLB) method*, and that from Giessen / Darmstadt [17], which is named *in-beam method*, is performed at the West German Proton Therapy Centre Essen (WPE) (Essen). As a third method, a measurement using a commercial PET scanner is performed. Furthermore, different experimental parameters that are suspected to potentially introduce systematic uncertainties (irradiation field geometry, target thickness, target material, target size, field size of the broad proton field) are varied for the DLB method.

2 Current status in the literature

Figure 1 shows an overview of the ^{nat}C(p,x)^{11}C cross section data sets currently found in literature [1,2,5,6,10,13,16–18,21,25,26]. Note, that the dataset by Kettern et al. [20] is not shown because the data points scatter strongly. The data points accumulate around two different curves. In many of the quoted publications only the relative error is given and systematic uncertainties have not been estimated properly. Therefore, due to this lack of standardization, the error-bars are not shown in Fig. 1. A detailed study of the original publications reveals that most measurements are only relative measurements normalizing on prior publications. Only five publications, Aamodt et al. [1], Kavanagh et al. [18], Kettern et al. [20], Bäcker et al. [5] (together with Bäumer et al. [6]), and Horst et al. [17] provide absolute measurements at 100 MeV beam energy. While Aamodt et al. [1] and Bäcker et al. [5] accumulate around the upper curve, Kavanagh et al. [18] and Horst et al. [17] accumulate around the lower one. The cross sections proposed by Kettern et al. [20] are in agreement with both curves because of the larger uncertainty of the experimental setup.

In the right panel of Fig. 1 the same data sets are normalized to 100 MeV (normalization done by extrapolation to 100 MeV). In the peak area between 50 and 60 MeV beam energy, the data points of some of the literature references scatter. This leads to possible uncertainties in the estimation of the exact trend of the excitation function. However, the shape of a sharp peak is highly likely based on the different literature sources. The normalization demonstrates that all past experiments have in fact measured the same curve of the ^{nat}C(p,x)^{11}C excitation function while the discrepancies between the measurements are found in the absolute cross-section values. Therefore, we report a detailed experimental study of the absolute cross section for the ^{nat}C(p,x)^{11}C reaction at 100 MeV. This value can then in turn be used to obtain a more reliable absolute excitation function from the relative values that are shown in the right panel of Fig. 1.

3 Materials and methods

In recent measurements of absolute ^{nat}C(p,x)^{11}C cross sections, two types of experimental methods have been developed, the DLB method [5,6] and the in-beam method [17]. Both methods are compared in a joint experiment performed at WPE. While the DLB experiment features a low-level gamma-ray spectrometry laboratory at the TU Dortmund University which requires the transport of the target from the proton therapy center to Dortmund (about 40 km), the in-beam method bases on an experimental setup to measure the activity of the targets directly at the beam line after the end of irradiation. Only important aspects for the comparison of the two methods are summarized in the following while details can be found in the original publications.

3.1 Proton therapy center

All irradiations for this study are performed at the WPE. The WPE is a cyclotron-based proton therapy center with four treatment rooms featuring a variety of delivery modes for clinical patient treatment. The pencil beam scanning technique is chosen for the experiments as it allows to use quasi mono-energetic proton beams with less secondary particles compared to passive beam applications techniques. The proton energy used for the present experiments is 100 MeV since most data from the past overlap at about 100 MeV and the activation cross section obtained by Kavanagh et al. [18], which is considered the gold standard, as the cross section is published with low uncertainties, has been measured at 98 MeV.

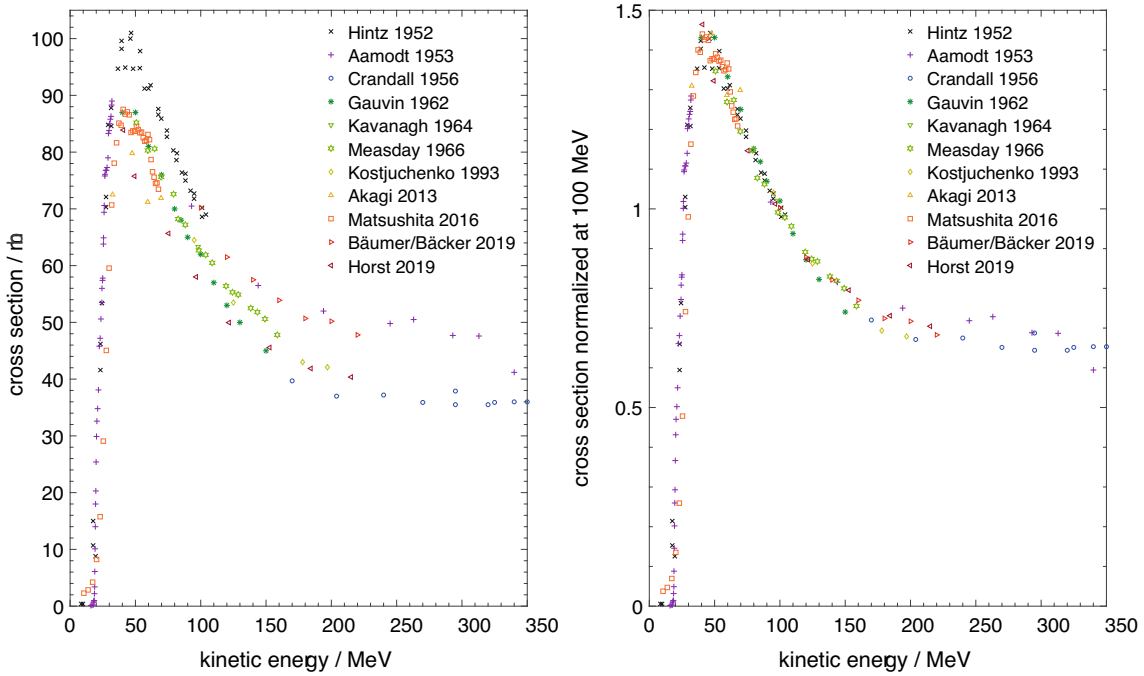

Fig. 1 Experimental cross sections for the $^{nat}C(p,x)^{11}C$ reaction found in the literature [1,2,5,6,10,13,16–18,21,25,26] as absolute values (left panel) and re-normalized to 100 MeV (right panel). No error bars are plotted because the uncertainties given in the literature are not consistent

3.2 Comparison of the induced activity measured by two different methods

In a first step, it is necessary to exclude any systematic errors in the initial ^{11}C activity determination with the two experimental setups. Therefore, a combined measurement is performed at the WPE. The in-beam setup known from Ref. [17] is installed at the WPE. The setup is based on three BaF_2 crystal scintillation detectors and a coincidence unit and is placed directly at the beam line downstream of the treatment head. Thus, it is possible to start the data acquisition directly after the irradiation is finished. The irradiation of the target is performed with a co-axial spot and the target is tilted by 45° compared to the beam axis, to achieve a better detection efficiency. The target has a lateral size of $(8.00\pm0.05)\times(8.00\pm0.05)\,cm^2$ and a thickness of (7.1 ± 0.1) mm in beam direction. The density is (1.8 ± 0.1) g/cm^3. The target material is manufactured from the same supplier of the target material as in Refs. [6,17] (SGL Carbon, Wiesbaden, Germany). Thus, impurities are considered to be negligible.

After the activation of the graphite target by a short proton pulse (shorter than 1 s), the in-beam setup immediately monitors the decay of the induced β^+-activity. It consists of three BaF_2 scintillators coupled by a coincidence trigger unit. Two scintillators are arranged in 180° to monitor the 511 keV photon coincidences from the β^+-decays of the produced ^{10}C and ^{11}C. A third scintillator is arranged at 90° to monitor the random coincidence rate which has to be subtracted from the 180° coincidences to obtain the true coincidence rate. For absolute calibration of the system, a ^{22}Na reference source as used in Ref. [17] is measured right before the experiment. To cross check the calibration, the ^{22}Na source from Ref. [6] is used in addition.

After about 20 min of data acquisition, the target is brought to the Dortmund Low Background Facility (DLB) to perform a gamma-ray spectrometry measurement. The distance between WPE and DLB is about 40 km resulting in about 40 min for the target transport. The experimental procedure is analogous to Ref. [5,6] and the initial ^{11}C activity is determined according to DIN ISO 11929:2011 [11]. The DLB is a low-level gamma-ray spectrometry laboratory at TU Dortmund University [12]. The laboratory is located above ground and has a multi-layer shielding with an active muon-veto to reduce the background down to approximately 1.85 counts/(min $kg_{detector}$) in the energy range from 40 to 2700 keV [29]. The detector itself is an about 1.2 kg high-purity germanium detector. Because of the sophisticated shielding concept, it is still possible to accurately determine activity even after the measurement at the beam line and the transport from Essen to Dortmund.

Previous activation experiments at the WPE have been performed with a scanned field larger than the target [5,6], while the in-beam setup [17] can only be used with a pencil beam impinging at the center of the target. For the comparative measurement of the in-beam and DLB method, it is

necessary to change the irradiation setup from the previous irradiations at the WPE and the subsequent activation measurements at the DLB to a pencil beam.

3.3 Variation of experimental parameters

After the direct comparison of both experimental setups, additional experimental parameters are investigated. While the number of incident protons, the target material (different densities, different suppliers) and field and target size have been investigated in a previous study and an influence was demonstrated to be insignificant [6], now, the target thickness, lateral target size and the irradiation technique (central axis pencil beam and scanned field) are compared. Therefore, targets of various thicknesses are irradiated with a co-axial pencil beam spot and a scanned proton field, which is larger by a factor of four compared to the lateral target size, to make sure that the target is activated homogeneously in lateral directions. Therefore, the lateral beam profile has been obtained by the so-called pair-magnification method introduced by Lin et al. [22,23] and optimized at the WPE [34]. The measurement is performed with an IBA Lynx PT (IBA Dosimetry, Schwarzenbruck, Germany). The Lynx PT detector features a scintillation screen of $30\times30\,\mathrm{cm}^2$ and a CCD chip to take an image of the scintillation light. For a target of $2.5\times2.5\,\mathrm{cm}^2$ and a beam energy of 100 MeV 28% of the protons miss the target which must be taken into account in the analysis. For the $8\times8\,\mathrm{cm}^2$ target from Sect. 3.2, the correction for lateral loss of protons is only 1.5%. Additionally, a $7.5\times7.5\,\mathrm{cm}^2$ large target with a significant larger thickness (15 mm) is irradiated with a single pencil beam. For this target, the correction is 0.9%, as the target is placed perpendicular to the beam direction. In contrast to the target used in Sect. 3.2, the targets used for the experiments described in this section are perpendicular to the beam axis during the irradiation. The obtained fluence profiles are shown in Fig. 2. It is visible, that a part of the protons, depending on the lateral size of the target does not hit the target for the single pencil beam irradiation. This has to be taken into account for the calculation of the activation cross section. The activation of the target holder for the scanned field does not affect the results of the activity measurement, as the target is extracted from the target holder before the activity is measured.

The uncertainties of the cross section measurements are estimated according to the description in Ref. [6]. Briefly, the systematic uncertainties originate from measurements of the number of protons using the Faraday-cup, gamma-ray spectrometry method, and the determination of the target mass. All uncertainties sum up to about 2.4% [6] (1 standard uncertainty). As increasing target thicknesses lead to decreasing proton energies, the activation is not homogenous in beam direction according to the increasing cross section shown in Fig. 1. For the correction of the beam profile for the single spot activation and for the inhomogeneous activation for targets thicker than 1 mm an additional 1% uncertainty has been estimated for the efficiency calculation of the gamma-ray spectrometer. In consequence, for these targets the uncertainty is 2.6% if only one correction is applied or 2.8% if both corrections are necessary.

For the activation with the scanned proton field, the activation cross section is calculated with the equation from Ref. [5]:

$$\sigma = \frac{M_\mathrm{T} A_0}{N_\mathrm{A} m_\mathrm{T} \Phi_\mathrm{proton} \lambda}. \tag{1}$$

A_0 is the decay-corrected activity for the time of irradiation, N_A is the Avogadro constant, M_T and m_T are the target's molar mass and mass, Φ_proton is the proton fluence (number of protons per field size) and $\lambda = 567.3 \cdot 10^{-6}\,1/\mathrm{s}$ [27] is the decay constant, calculated from the half-life of ^{11}C. For the single spot activation the cross section is calculated according to Ref. [17]:

$$\sigma = \frac{A_0}{z \frac{n}{V} N \lambda}, \tag{2}$$

where z is the target thickness, N is the corrected number of protons across the target area and $\frac{n}{V}$ is the particle density of the target. The correction for the number of protons is calculated from the fluence distributions obtained with the Lynx PT described at the beginning of this section. Using conversions, it can be shown that both equations are equivalent. Both equations contain the accessible variables for the number of protons, number of reaction products and number of target nuclei for each experiment.

3.4 Validation measurements with a PET/CT scanner

To check the consistency of all performed measurements, two additional measurements are performed using a Siemens Biograph Vision ToF-PET/CT System (Siemens Healthineers, Erlangen, Germany). For the first measurement a 10 cm large stack of $2.5\times2.5\,\mathrm{cm}^2$ 1 mm thick graphite foils is activated with a scanned field of 130 MeV protons. At 3.7 cm depth, the graphite is activated by protons with an average residual energy of 100 MeV. However, the energy spread of the degraded beam is larger than for the irradiations presented in Sects. 3.2 and 3.3. The activity of the complete stack is measured with the PET scanner and the cross section is calculated with this result.

The second measurement is the activation of a larger target ($5\times5\,\mathrm{cm}^2$) with a single pencil beam directed to the center of the target. The target is divided into four sections. Each section has a different thickness consisting of one, three, five and seven 1 mm thick graphite sheets. In consequence, different activities are obtained for the sections. Furthermore,

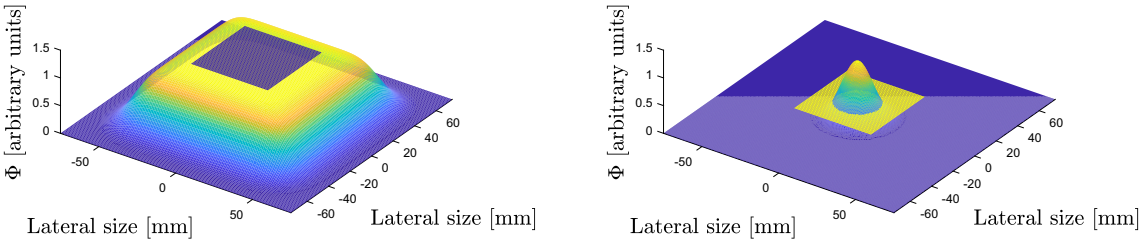

Fig. 2 Left: Calculated fluence distribution of the scanned proton field with 21 × 21 spots (measured one single spot profile) and the target area (blue). Right: Measured fluence distribution of a single spot activation with target area (yellow)

the lateral profile of the activation is obtained with the measurement.

Before starting with the experiment, the calibration of the PET scanner is checked with the ^{22}Na-source used for the cross check of the in-beam setup and in Ref. [6]. The measurement results in a precision of 5% of the estimation of the activity. The 5% deviation from the calibration certificate of the source is the assumed systematic uncertainty of the PET system, which is commonly taken in clinical practices [19].

4 Results and discussion

4.1 Comparison of the activity determined with the two experimental setups

The β^+ activities induced in a graphite target irradiated with 5×10^9 protons are measured with both experimental setups. To compare the determined initial activities, the exponential decay of the ^{11}C has to be taken into account, since the target has to be brought from Essen to Dortmund for the measurement at the DLB. The decay curve obtained with the coincidence setup at the beam line and at the DLB in the annihilation peak of the gamma-ray spectrum is shown in Fig. 3. It is visible, that both activities match within their uncertainties. The activity obtained at the beam line is $A_0^{\text{in-beam}} = (11.1 \pm 0.7)$ kBq. The activity obtained at the DLB is $A_0^{\text{DLB}} = (11.7 \pm 0.4)$ kBq. The uncertainty of the DLB is lower compared to the in-beam setup which is given by the special design and characteristics of the DLB. Moreover, within the first seconds of the measurement, a fast decay of produced ^{10}C is visible. It is not measured at the DLB due to the short half-life. Once, the cross sections for the productions of ^{11}C has been validated, previous measurements of the cross section for the ^{10}C production can be reviewed as well.

Data acquisition time at the DLB is about 2 weeks, to identify possible impurities in the graphite target, as they have been found in a previous study [6]. A gamma-ray spectrum of the activated graphite sample is shown in Fig. 4. Compared to

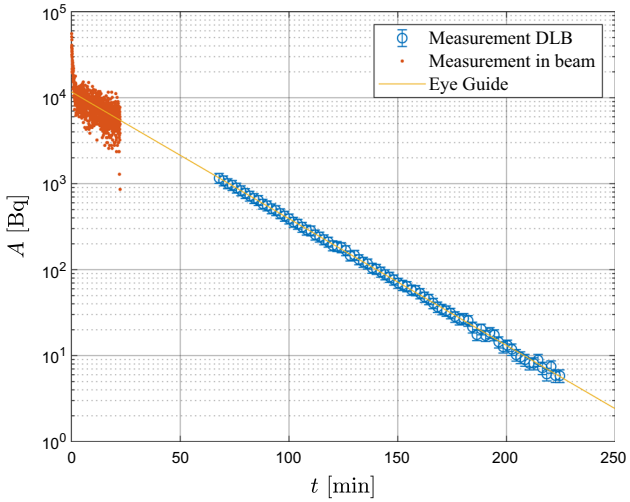

Fig. 3 Visualization of the activities obtained with the in-beam setup and at the DLB. The gap is due to the time for the transport of the target (approx. 40 min)

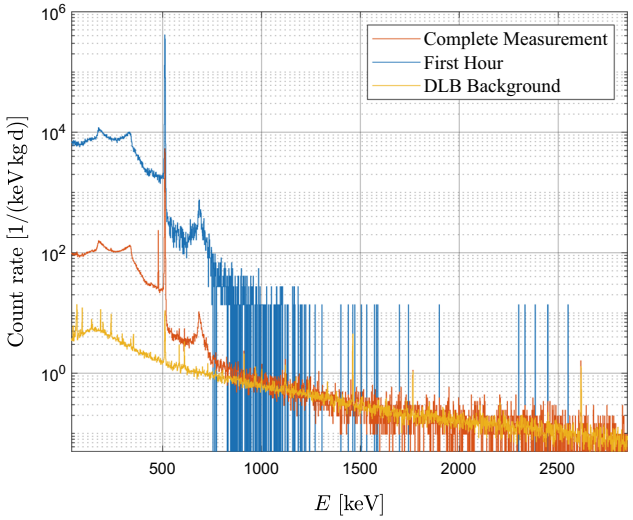

Fig. 4 Gamma-ray spectrum of the first hour of the measurement (blue) and the complete measurement (red, about 12 days) with the background spectrum of the DLB (yellow). Two peaks can be obtained in the measurement, the annihilation peak from ^{11}C and the one at 478 keV from ^{7}Be

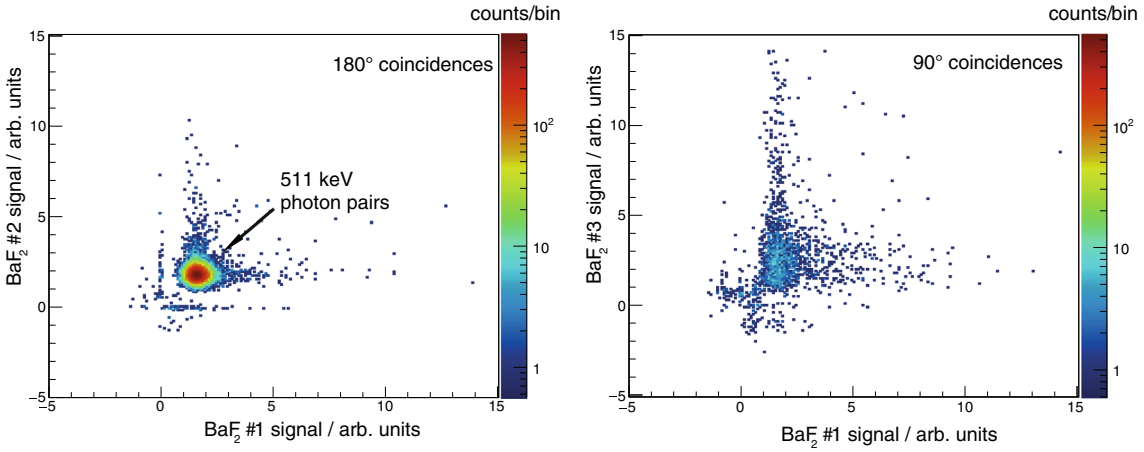

Fig. 5 In-beam method: Energy spectra of the coincidence events detected by the 180° detector pair (left panel) and random coincidences detected by the 90° detector pair (right panel) from the graphite target activated by 100 MeV protons

previous studies, no peaks are visible in the spectrum which indicate such impurities. The ^{7}Be is produced from carbon as well, but due to the smaller number of impinging protons and short time of measurement compared to Ref. [5] the statistical uncertainty is larger and the radionuclide is not analyzed here. Within the first hour an additional coincidence peak of the full energy peak and the back-scatter peak of the 511 keV photons is visible at approximately 700 keV. The influence of the coincidence of a primary 511 keV photon and a back-scattered photon on the estimated activity is insignificant as the peak is smaller by three orders of magnitude.

Figure 5 shows the energy spectra of the events detected by the 180° and by the 90° detector pairs obtained with the in-beam setup. In an offline analysis, the 511 keV peaks are separated by applying a cut on the energy spectra. Subtracting the 90° coincidences from those measured in 180° gives the true 180° coincidence rate required for determination of the initial activity.

4.2 Variation of experimental parameters and measurements at the DLB

Several targets with different densities and thicknesses are irradiated with a single pencil beam and a scanned proton field. From the measured activity of ^{11}C, the activation cross section is calculated. Table 1 provides an overview on the experimental parameters and the results of the activation cross section determination. All results are shown in Fig. 6 for comparison. Since the targets have different densities and thicknesses, the areal density $z\rho$, where ρ is the density of the target material, is considered to be a representative for the effective thickness of the targets. For $z\rho$ less than 1 g/cm^2 the calculated activation cross sections vary between 67 and 70 mb and agree within one standard deviations. For $z\rho > 1$ g/cm^2, the calculated cross sections are slightly smaller, but an increasing cross section is expected because of the degradation of the beam energy of 7 MeV in 1.5 g/cm^2 graphite [7]. However, the correction of the efficiency of the DLB is less accurate for increasing $z\rho$ because the activation increases with the thickness of the targets as the cross section increases at lower energies (see Fig. 1). This results in an increasing activity to the downstream end of the target. The targets are placed with the upstream end of the target on the detector end-cap. In consequence, the slight decrease of the measured cross section might be induced by systematic uncertainties of the estimated activity profile for the efficiency calculation. In contrast, Kavanagh et al. [18] observed an increasing cross section for thicker target, but the thickness of the target ranged between 0.15 and 0.65 cm and no information on the density is given. Furthermore, the increase is about 1 mb which is well below the differences measured in the current study. However, a plastic scintillator has been used as target material. Today, high-purity graphite sheets are supposed to be superior compared to plastic targets as used in the past.

Additionally, the agreement of all measurements can be tested in an alternative way. The activation cross section is representative of the probability of the nuclear reaction. Independent from the target size, $z\rho$ is representative of the number of target nuclei for a homogenous distribution of the target particles across the target area. The number of activated residuals per number of incident protons gives the probability of a reaction in each target. For a constant activation cross section for all $z\rho$, all measurements of the study should accumulate around a linear fit, which slope represents the activation cross section. In Fig. 7, it is visible, that indeed all measurements accumulate around a linear fit. The activation cross section calculated from the slope is (67.0 ± 1.8) mb. This value is smaller than the mean value of all values. As it is visible in the Figs. 6 and 7, the cross sections for $z\rho > 1.0$ g/cm^2 are

Table 1 Measurement results for the calculation of the activation cross sections for the $^{nat}C(p,x)^{11}C$-reaction at 100 MeV for the different targets. "hd" indicates high-density target material used in the experiments described in Ref. [17], "ld" low-density for the target material used in the experiments described in Refs. [5,6]. The value for the scanned-field activation of the ld-target is taken from Ref. [6]. The correction is the correction for the lateral beam profile. [1]This result is obtained with the in-beam setup, same target and activation as line before

Irradiation	target	$z\rho$ [g/cm^2]	Correction	Lateral size [cm^2]	Measured cross section [mb]
Scanned	ld	0.099	No	2.5×2.5	70.2 ± 1.7
Scanned	hd	0.180	No	2.5×2.5	70.4 ± 1.5
Scanned	hd	0.540	No	2.5×2.5	67.4 ± 1.6
Scanned	hd	0.900	No	2.5×2.5	69.1 ± 1.6
Spot	ld	0.099	28%	2.5×2.5	69.7 ± 1.7
Spot	ld	0.099	28%	2.5×2.5	69.4 ± 1.7
Spot	hd	0.180	28%	2.5×2.5	68.6 ± 1.8
Spot	hd	0.540	28%	2.5×2.5	67.3 ± 1.7
Spot	hd	0.900	28%	2.5×2.5	68.4 ± 1.8
Spot, tilted	hd	1.278	1.5%	8.0×8.0	64.7 ± 1.7
Spot, tilted[1]	hd	1.278	1.5%	8.0×8.0	61.5 ± 7.0
Spot	ld	1.424	0.9%	7.5×7.5	66.6 ± 1.7

smaller than the other activation cross sections obtained at the DLB. Thus, these individual results have a large influence on the result of the fit. The deviation is explained by the uncertainty of the efficiency of the DLB. For the targets with $z\rho < 1.0\,\mathrm{g/cm^2}$, (68 ± 3) mb is concluded as the reference cross section as this is the mean of all obtained activation cross sections. As the beam is degraded along the target, (97 ± 3) MeV is the reference energy of the calculated cross section.

4.3 Consistency measurements with a PET/CT

In the PET image, a region of interest (ROI) is placed 4 mm around the point where the proton beam is degraded to 100 MeV. The activity of the ROI is measured and subsequently the activation cross section is calculated as (69.8 ± 3.6) mb. This experiment is a test, if thick targets may result in a bias determining the activation cross sections. The calculated activation cross section is in the same magnitude as the ones presented in Sect. 4.3 and added to Fig. 6. The uncertainty is given by the one of the PET scanner (5%). Obviously, this simple study does not result in a high accuracy measurement for cross section determination compared to the gamma-ray spectrometry with a high-purity germanium detector. Furthermore, more uncertainties have to be taken into account, like the energy loss straggling of the protons or the scattered protons, which leave the target. All further uncertainties result in less accuracy of this measurement method. In consequence, the uncertainty of the determined cross section is larger than the 5% contribution of the activity and the 1.1% of the number of protons [6].

In a second step, a target with varying thicknesses is irradiated with a single pencil beam. For the four sections of the

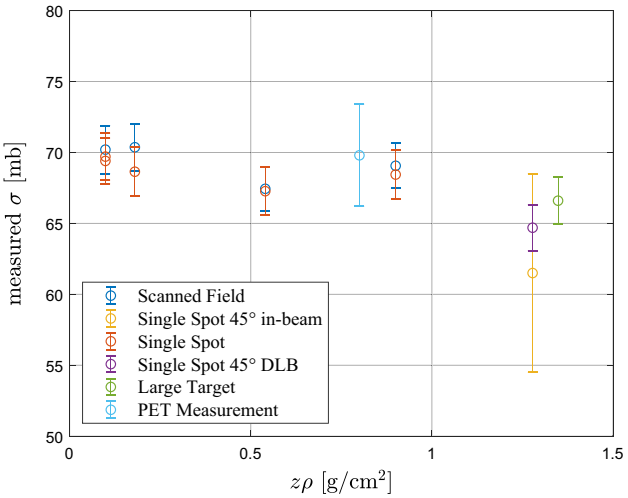

Fig. 6 Activation cross section obtained for the different targets and techniques. Blue: scanned field with small targets. Red: single-spot activation with small targets, results corrected for beam profile. Yellow: Cross section obtained with the in-beam setup with a tilted angle, lateral profile corrected. Purple: Measurement of the same target at the DLB. Green: Large stack of graphite sheets. The light blue result is from the PET measurement, see Sect. 4.2

targets (one, three, five and seven sheets) a linear increase of the produced activity is obtained in the measurement. This observation is difficult to obtain with the gamma-ray spectrometry due to the self-absorption and geometric effects, – especially a decreasing sensitivity with increasing distance to the detector. The obtained linear increase of the activity determined with the PET confirms, that the chosen assumption to correct for different effects in Sect. 4.2 is plausible.

In summary, both studies with the PET scanner are in agreement with the results presented in Sect. 4.2 and a new

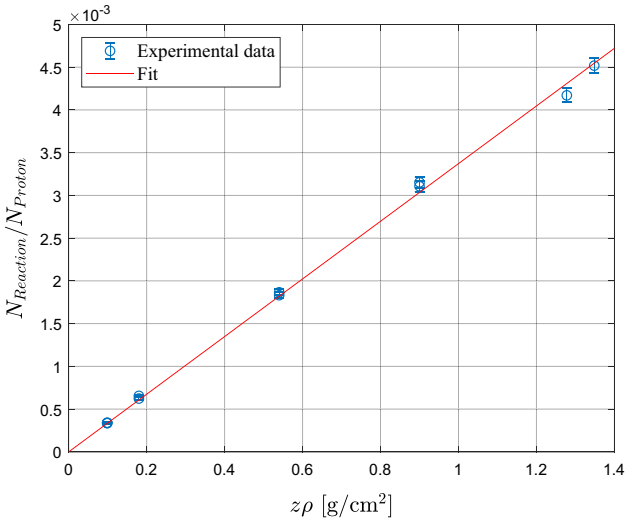

Fig. 7 Reaction probability increases with the effective target thickness. Only DLB measurements are shown in the plot. A linear model is fitted to the data

reference cross section can be derived from the measurements performed at the DLB.

4.4 Renormalization of the excitation function

All experimental parameters included in the study can be ruled out as the cause of the systematic difference among past publications as all results from both experiments described in this paper converge at one value. Thus, another experimental parameter has to be the origin of the systematic deviation of the measured cross sections.

The experimental setups used in the latest publications have been compared with a joint experiment, analyzing the same target with the in-beam and the DLB method. After a systematic error of one of the measurement setups has been excluded, the experimental parameters have been varied. The activity of the targets has been measured with the well-known gamma-ray spectrometry setup DLB. In summary, it is possible to reduce the systematic uncertainties down to 3%. From the measured cross sections presented in Sects. 4.2 and 4.2, (68±3) mb is derived as the new reference cross section for (97±3) MeV protons as the weighted mean value of all measured cross section in this work. The different relative uncertainties are used as the weights, to consider the different accuracy of the individual experimental setups. The energy of (97±3) MeV is given by the degradation of the beam in the thick targets used in the experiments. The new reference value is shown in Fig. 8 together with several values obtained from the literature [1,5,6,13,16–18,21,26]. The proposed reference value presented in this work is in agreement with all previous values within their uncertainties.

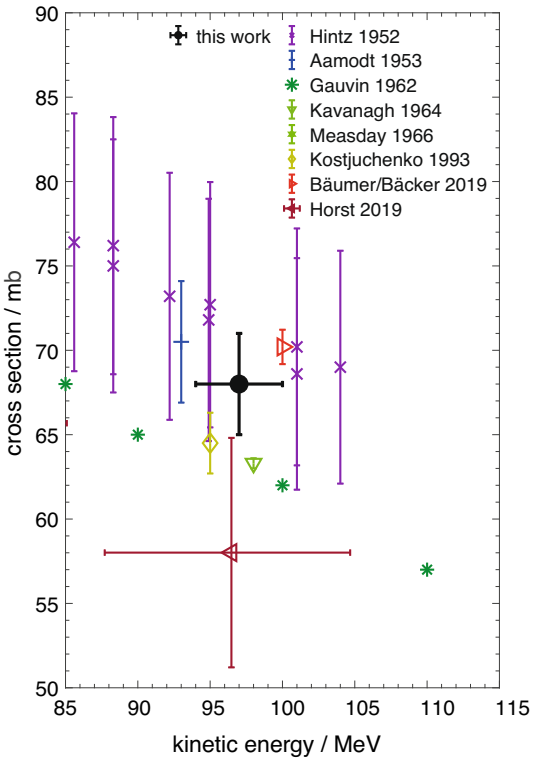

Fig. 8 Absolute cross section from the literature with their uncertainties [1,5,6,13,16–18,21,26] together with the new proposed reference cross section

From the results in Sect. 4.2, it can be derived that thin targets should be used for cross sections measurements as the results for the thin targets scatter less than the one for thicker targets. Thin targets manipulate the beam less than thick targets and the properties of the beam can be assumed to be constant. With a well defined proton beam at a clinical therapy center, the targets can be irradiated with different irradiation techniques. In addition, the consistency check with the PET scanner results in a comparable cross section. This third independent method excludes any error for both setups, the in-beam setup and the DLB. A thicker target and a build-up is used in the PET scanner. This results in higher uncertainties for the measured cross section. The linear increase of the activity by increasing the thickness of a target is demonstrated as well, as shown in Fig. 7. However, at some point thick targets will lead to an inaccuracy of the cross sections measurement due to difficult accessible beam properties. With the new reference cross section, the normalized excitation function presented in the right panel of Fig. 1 can be re-normalized to this value. With the normalized data given in the supplementary material, a new excitation function can be calculated. After the re-normalization of the $^{nat}C(p,x)^{11}C$ excitation function, more cross sections for other nuclear reactions can be reviewed whether a re-

normalization is necessary, since many literature values have been measured relative to this cross section.

At last, there is a potential difference to the cross section published in Ref. [17]. To explain this difference, it has to be mentioned that two different methods for determining the primary proton number are commonly applied: by means of a dose measurement using an ionization chamber or by means of a charge measurement using a Faraday cup, e.g. Refs. [8,9,14]. A systematic difference of up to 3% has been observed along the publications over time, where Faraday cup measurements result in a higher number of incident protons. Furthermore, systematic uncertainties of these translate directly into the cross section value and it is yet unclear which method is more accurate. Both methods are still under investigation and possible systematic errors are discussed in the literature aiming for the correct results, see e.g. Refs. [24,30]. For all cross section calculations presented in this study, a Faraday cup based monitor calibration is used, as it is common for nuclear physics experiments. As presented in Ref. [6], the Faraday cup measurement has been performed according to [15].

In conclusion, we want to note that the observed 3% difference between both measurement methods to determine the number of protons is covered in our uncertainty. While the Faraday Cup measurement is associated with an uncertainty of about 1.2% [6], the reference dosimetry in proton therapy using ionization chambers is associated with an uncertainty of 2.3% according to IAEA TRS 398 [3]. However, further studies on the difference of both methods might reduce the uncertainty of the cross sections further.

5 Conclusion

The presented study investigates the $^{nat}C(p,x)^{11}C$ reaction at a proton energy of 100 MeV. The previously published activation cross sections scatter by about 15%. The experimental parameters and the two recent measurements of activation cross sections are investigated regarding their influence on the obtained results. In result, all investigated parameters do not have any influence on the measured cross section on a significant level. With a well-defined gamma-ray spectrometer system and varying the several experimental parameters and an additional validation measurement with a PET scanner, the cross section is measured with a high accuracy. A new reference value of (68 ± 3) mb is provided at (97 ± 3) MeV proton energy, which gives together with the re-normalized literature data accurate values of the absolute $^{nat}C(p,x)^{11}C$ excitation function in the energy range relevant for proton therapy. This allows an accurate modeling of the $^{nat}C(p,x)^{11}C$ nuclear reaction and calculation of PET activity distributions in proton therapy patients. Other cross section data from the literature can be reviewed if they have been measured relative to the carbon activation in the past. Moreover, Monte Carlo simulations of activity distributions will benefit from more accurate cross-section data. However, a remaining issue for determination of an accurate absolute cross section is the relatively high uncertainty of the beam monitor calibration. Systematic differences between the two standard methods in proton therapy, based on either Faraday cup or ionization chamber measurements, of up to 3% are an open issue. For this study, the Faraday cup is supposed to be the more accurate estimation of the number of protons as it is common in nuclear physics experiments.

Acknowledgements The presented study was supported by the MERCUR-Stiftung graduate school "Präzisionsprotonentherapie – Praxisbezogene Physik und Chemie an der Schnittstelle zur Medizin" (Grant number St-2019-0007). The authors would like to thank Andrija Matic, Ryan Swanson and Ben Liu from IBA PT and the WPE physics team for their support with the target irradiation as well as Miriam Niekämper from the Ruhr University Bochum for the discussion about details in the original French publications.

Funding Open Access funding enabled and organized by Projekt DEAL.

Data Availability Statement This manuscript has no associated data or the data will not be deposited. [Authors' comment: The data contain clinical confident information which cannot be published.]

Declarations

Conflict of interest The authors declare that they have no conflict of interest.

References

1. R.L. Aamodt, V. Peterson, R. Phillips, C^{12}(p, pn)C^{11} cross section from threshold to 340 MeV. Phys. Rev. **88**(4), 739–744 (1952). https://doi.org/10.1103/PhysRev.88.739
2. T. Akagi, M. Yagi, T. Yamashita, M. Murakami, Y. Yamakawa, K. Kitamura, K. Ogura, K. Kondo, S. Kawanishi, Experimental study for the production cross sections of positron emitters induced from 12C and 16O nuclei by low-energy proton beams. Radiat. Meas. **59**, 262–269 (2013). https://doi.org/10.1016/j.radmeas.2013.07.005
3. P. Andreo, D.T. Burns, K. Hohlfeld, M.S. Huq, T. Kanai, F. Laitano, V. Smyth, S. Vynckier, Absorbed Dose Determination in External Beam Radiotherapy Technical Reports Series No. 398, v.12 edn. International Atomic Energy Agency, Vienna (2006)

4. A. Aricò, G. Battistoni, F. Cerutti, F. Horst, A. Mairani, C. Schuy, U. Weber, A. Ferrari, Benchmarking of FLUKA production cross sections of positron emission tomography isotopes for in-vivo range verification in hadron therapy. EPJ Web Conf. **239**, 24001 (2020). https://doi.org/10.1051/epjconf/202023924001
5. C.M. Bäcker, C. Bäumer, M. Gerhardt, K. Kröninger, C. Nitsch, H.M. Siregar, B. Timmermann, N. Verbeek, J. Weingarten, J. Wulff, A. Yazgan, Measurement of nuclear activation cross section of protons on natural carbon from proton beam energies between 100 and 220 mev. Nucl. Inst. Methods Phys. Res. B **454**, 50–55 (2019). https://doi.org/10.1016/j.nimb.2019.06.011
6. C. Bäumer, C.M. Bäcker, M. Gerhardt, E. Grusell, B. Koska, K. Kröninger, C. Nitsch, H. Rullkötter, H. Siregar, B. Timmermann, N. Verbeek, J. Wulff, A. Yazgan, Measurement of absolute activation cross sections from carbon and aluminum for proton therapy. Nucl. Inst. Methods Phys. Res. B **440**, 75–81 (2019). https://doi.org/10.1016/j.nimb.2018.11.020
7. M. Berger, J. Coursey, M. Zucker, J. Chang, Stopping-power & range tables for electrons, protons, and helium ions 2017. https://physics.nist.gov/PhysRefData/Star/Text/PSTAR.html. NIST Standard Reference Database 124 (2017)
8. R. Cambria, J. Hérault, N. Brassart, M. Silari, P. Chauvel, Proton beam dosimetry: a comparison between the Faraday cup and an ionization chamber. Phys. Med. Biol. **42**(6), 1185–1196 (1997). https://doi.org/10.1088/0031-9155/42/6/014
9. B. Clasie, N. Depauw, M. Fransen, C. Gomà, H.R. Panahandeh, J. Seco, J.B. Flanz, H.M. Kooy, Golden beam data for proton pencil-beam scanning. Phys. Med. Biol. **57**(5), 1147–1158 (2012). https://doi.org/10.1088/0031-9155/57/5/1147
10. W.E. Crandall, G.P. Millburn, R.V. Pyle, W. Birnbaum, C^{12}(x, xn)C^{11}andAl^{27}(x, x2pn)Na^{24} Cross sections at high energies. Phys. Rev. **101**, 329–337 (1956). https://doi.org/10.1103/PhysRev.101.329
11. Deutsches Institut für Normung, Berlin: DIN ISO 11929 Januar 2011: Bestimmung der charakteristischen Grenzen (Erkennungsgrenze, Nachweisgrenze und Grenzen des Vertrauensbereichs) bei Messungen ionisierender Strahlung – Grundlagen und Anwendungen (2011)
12. H. Gastrich, C. Gößling, R. Klingenberg, K. Kröninger, T. Neddermann, C. Nitsch, T. Quante, K. Zuber, The Dortmund low background facility—low-background gamma ray spectrometry with an artificial overburden. Appl. Radiat. Isot. **112**, 165–176 (2016). https://doi.org/10.1016/j.apradiso.2016.03.025
13. H. Gauvin, M. Lefort, X. Tarrago, Émission d'hélions dans les réactions de spallation. Nucl. Phys. **39**, 447–463 (1962). https://doi.org/10.1016/0029-5582(62)90403-0
14. C. Gomà, S. Lorentini, D. Meer, S. Safai, Proton beam monitor chamber calibration. Phys. Med. Biol. **59**, 4961–4971 (2014). https://doi.org/10.1088/0031-9155/59/17/4961
15. E. Grusell, U. Isacsson, A. Montelius, J. Medin, Faraday cup dosimetry in a proton therapy beam without collimation. Phys. Med. Biol. **40**(11), 1831–1840 (1995). https://doi.org/10.1088/0031-9155/40/11/005
16. N.M. Hintz, N.F. Ramsey, Excitation functions to 100 MeV. Phys. Rev. **88**(1), 19–27 (1952). https://doi.org/10.1103/PhysRev.88.19
17. F. Horst, W. Adi, G. Aricò, K.T. Brinkmann, M. Durante, C.A. Reidel, M. Rovituso, U. Weber, H.G. Zaunick, K. Zink, C. Schuy, Measurement of PET isotope production cross sections for protons and carbon ions on carbon and oxygen targets for applications in particle therapy range verification. Phys. Med. Biol. (2019). https://doi.org/10.1088/1361-6560/ab4511
18. T.M. Kavanagh, J.K.P. Lee, W.T. Link, A precise measurement of the C^{11} production cross section for 98-MeV protons on carbon. Can. J. Phys. **42**(8), 1429–1436 (1964). https://doi.org/10.1139/p64-130
19. S.H. Keller, B. Jakoby, S. Svalling, A. Kjaer, L. Højgaard, T.L. Klausen, Cross-calibration of the Siemens mMR: easily acquired accurate PET phantom measurements, long-term stability and reproducibility. Eur. J. Nucl. Med. Mol. Imaging Phys. **3**, 11 (2016). https://doi.org/10.1186/s40658-016-0146-3
20. K. Kettern, Y.N. Shubin, G.F. Steyn, T.N. van der Walt, H.H. Coenen, S.M. Qaim, Formation of short-lived positron emitters in reactions of protons of energies up to 200 MeV with the target elements carbon, nitrogen and oxygen. Appl. Radiat. Isot. **60**(6), 939–945 (2004). https://doi.org/10.1016/j.apradiso.2004.02.007
21. V. Kostjuchenko, D. Nichiporov, Measurement of the $^{12}C(p, pn)^{11}C$ reaction from 95 to 200 MeV. Appl. Radiat. Isot. **44**(9), 1173–1175 (1993). https://doi.org/10.1016/0969-8043(93)90060-N
22. L. Lin, C.G. Ainsley, J.E. McDonough, Experimental characterization of two-dimensional pencil beam scanning proton spot profiles. Phys. Med. Biol. **58**, 6193 (2013). https://doi.org/10.1088/0031-9155/59/2/493
23. L. Lin, C.G. Ainsley, T. Mertens, O.D. Wilde, P.T. Talla, J.E. McDonough, A novel technique for measuring the low-dose envelope of pencil-beam scanning spot profiles. Phys. Med. Biol. **58**, N171 (2013). https://doi.org/10.1088/0031-9155/58/12/N171
24. F. Luoni, U. Weber, D. Boscolo, M. Durante, C.A. Reidel, C. Schuy, K. Zink, F. Horst, Beam monitor calibration for radiobiological experiments with scanned high energy heavy ion beams at fair. Front. Phys. **8**, 397 (2020). https://doi.org/10.3389/fphy.2020.568145
25. K. Matsushita, T. Nishio, S. Tanaka, M. Tsuneda, A. Sugiura, K. Ieki, Measurement of proton-induced target fragmentation cross sections in carbon. Nucl. Phys. A **946**, 104–116 (2016). https://doi.org/10.1016/j.nuclphysa.2015.11.007
26. D.F. Measday, The $^{12}C(p, pn)^{11}C$ reaction from 50 to 160 MeV. Nucl. Phys. **78**(2), 476–480 (1966). https://doi.org/10.1016/0029-5582(66)90621-3
27. National Nuclear Data Center: information extracted from the nudat 2 database. http://www.nndc.bnl.gov/nudat2/. Accessed 30 July 2021
28. D. Nichiporov, Verification of absolute ionization chamber dosimetry in a proton beam using carbon activation measurements. Med. Phys. **30**(5), 972–978 (2003). https://doi.org/10.1118/1.1568591
29. C. Nitsch, M. Gerhardt, C. Gößling, K. Kröninger, Improvements to the muon veto of the Dortmund Low Background Facility. Appl. Radiat. Isot. **126**, 201–203 (2017). https://doi.org/10.1016/j.apradiso.2017.02.041
30. J. Osorio, R. Dreindl, L. Grevillot, V. Letellier, P. Kuess, A. Carlino, A. Elia, M. Stock, S. Vatnitsky, H. Palmans, Beam monitor calibration of a synchrotron-based scanned light-ion beam delivery system. Z. Med. Phys. (2020). https://doi.org/10.1016/j.zemedi.2020.06.005
31. N. Otuka, E. Dupont, V. Semkova, B. Pritychenko, A. Blokhin, M. Aikawa, S. Babykina, M. Bossant, G. Chen, S. Dunaeva, R. Forrest, T. Fukahori, N. Furutachi, S. Ganesan, Z. Ge, O. Gritzay, M. Herman, S. Hlavač, K. Kato, B. Lalremruata, Y. Lee, A. Makinaga, K. Matsumoto, M. Mikhaylyukova, G. Pikulina, V. Pronyaev, A. Saxena, O. Schwerer, S. Simakov, N. Soppera, R. Suzuki, S. Takács, X. Tao, S. Taova, F. Tárkányi, V. Varlamov, J. Wang, S. Yang, V. Zerkin, Y. Zhuang, Towards a more complete and accurate experimental nuclear reaction data library (EXFOR): International Collaboration Between Nuclear Reaction Data Centres (NRDC). Nucl. Data Sheets **120**, 272–276 (2014). https://doi.org/10.1016/j.nds.2014.07.065
32. K. Parodi, H. Paganetti, H.A. Shih, S. Michaud, J.S. Loeffler, T.F. DeLaney, N.J. Liebsch, J.E. Munzenrider, A.J. Fischman, A. Knopf, T. Bortfeld, Patient study of in vivo verification of beam delivery and range, using proton emission tomography and computed tomography imaging after proton therapy. Int. J. Radiat.

Oncol. Biol. Phys. **68**(3), 920–934 (2007). https://doi.org/10.1016/j.ijrobp.2007.01.063
33. J. Tobailem, C.H. de Lassus, Sections efficacies des réactions nucléaires induites par protons, deuterons, particules alpha. CEA (1971). CEA-N-1466(1)
34. N. Verbeek, J. Wulff, C. Bäumer, S. Smyczek, B. Timmermann, L. Brualla, Single pencil beam benchmark of a module for Monte Carlo simulation of proton transport in the PENELOPE code. Med. Phys. **48**(1), 456–476 (2021). https://doi.org/10.1002/mp.14598